Chem. Senses 37: 479–493, 2012

doi:10.1093/chemse/bjr130
Advance Access publication February 2, 2012

# Mammalian-Specific OR37 Receptors Are Differentially Activated by Distinct Odorous Fatty Aldehydes

**Verena Bautze[1], Raphaela Bär[1], Benjamin Fissler[1], Michaela Trapp[1], Dietmar Schmidt[2], Uwe Beifuss[2], Bernd Bufe[3], Frank Zufall[3], Heinz Breer[1] and Jörg Strotmann[1]**

[1]Institute of Physiology, University of Hohenheim, Garbenstrasse 30, 70593 Stuttgart, Germany, [2]Institute of Chemistry, University of Hohenheim, Garbenstrasse 30, 70593 Stuttgart, Germany and [3]Department of Physiology, University of Saarland, 66421 Homburg, Germany

*Correspondence to be sent to: Jörg Strotmann, Institute of Physiology, University of Hohenheim, Garbenstrasse 30, 70593 Stuttgart, Germany. e-mail: strotman@uni-hohenheim.de*

*Accepted December 20, 2011*

## Abstract

The capacity of the mammalian olfactory system to detect an enormous collection of different chemical compounds is based on a large repertoire of odorant receptors (ORs). A small group of these ORs, the OR37 family, is unique due to a variety of special features. Members of this subfamily are exclusively found in mammals, they share a high degree of sequence homology and are highly conserved during evolution. It is still elusive which odorants may activate these atypical receptors. We have reasoned that compounds from skin, hairs, or skin glands might be potential candidates. We have exposed mice to such compounds and monitored activation of glomeruli through the expression of the activity marker c-fos in juxtaglomerular cells surrounding ventrally positioned glomeruli in the olfactory bulb (OB). Employing this methodology it was found that stimulation with long-chain alkanes elicits activation in the ventral part of the OB, however, none of the OR37 glomeruli. Analyses of long-chain hydrocarbon compounds with different functional groups revealed that long-chain aliphatic aldehydes elicited an activation of defined OR37 glomeruli, each of them responding preferentially to an aldehyde with different chain lengths. These results indicate that OR37 receptors may be tuned to distinct fatty aldehydes with a significant degree of ligand specificity.

**Key words:** ligand, mouse, odorant receptor, olfaction

## Introduction

The capacity of the mammalian olfactory system to detect a vast number of structurally diverse odorous compounds is based on a large repertoire of odorant receptors (ORs) (Buck and Axel 1991). Macrosmatic species like mice possess more than a thousand different receptor subtypes, each encoded by an individual gene (Young and Trask 2002; Zhang and Firestein 2002; Godfrey et al. 2004; Malnic et al. 2004). This huge repertoire has evolved by a series of gene duplications (Ben Arie et al. 1994; Glusman et al. 1996; Sosinsky et al. 2000; Xie et al. 2000; Lane et al. 2001), driven by positive selection individual genes have incorporated mutations which led to amino acid changes, thereby creating an enormous sequence diversity and thus the receptor variability which is the basis for recognizing and discriminating a wide range of odor molecules. Olfactory sensory neurons (OSNs), which express the same OR, are typically widely scattered throughout the olfactory epithelium (OE) and their axons project to 2 specific glomeruli in the olfactory bulb (OB) (Ressler et al. 1993, 1994; Vassar et al. 1993, 1994; Strotmann et al. 1994; Mombaerts et al. 1996). Although these features—receptor diversity, scattered distribution of receptor-specific OSNs and the dual wiring pattern—appear to be the prevalent principle in the mammalian olfactory system, there is an exception from this rule. Genes encoding receptors of the so-called OR37 subfamily share a high degree of sequence homology to each other (Hoppe et al. 2003), which is even the case across species border (Hoppe et al. 2006). Thus, in contrast to the variability of most other ORs, the OR37 receptors are highly conserved. The proteins encoded by the OR37 genes differ structurally by an insertion of 6 amino acids in their third extracellular loop (Kubick et al. 1997). Moreover, OSNs, which express a member from

the OR37 subfamily, are not dispersed throughout one of the OR expressing zones in the OE but concentrated in a small patch (Strotmann et al. 1999). Finally, the OR37 neurons do not project to 2 glomeruli but target only a single glomerulus in the ventral domain (Strotmann et al. 2000). Phylogenetic analyses have shown that this unique OR37 type of receptor exists exclusively in mammalian species (Hoppe et al. 2006), suggesting that it may recognize compounds, which are particularly relevant for mammals. In this context, it is interesting to note that a characteristic feature of mammals is their hairy skin, which coincides with sebaceous glands that secrete waxy material (Thody and Shuster 1989). This sebum is a complex mixture of lipids, including long hydrocarbons with a mainly protective function for the skin and hair. It seems conceivable that some of the compounds on the body surface may serve as signaling molecules. Based on these considerations, we set out to explore whether OR37 receptors may be activated by such long-chain molecules.

## Materials and methods

### Experimental animals

The study was performed using our previously generated transgenic mouse strains, which carry targeted mutations of IRES-taulacZ or IRES-tauGFP at the mOR37A-, mOR37B- or mOR37C-locus (Strotmann et al. 2000). Animals were housed at the Central Unit for Animal Research at the University of Hohenheim. For tissue preparations, animals were killed by cervical dislocation or by $CO_2$ asphyxiation and subsequent decapitation as approved by the regional administrative authority.

### Odorants

Tetradecane and pentadecane were purchased from Acros organics, hexadecane from Fisher scientific, tetradecanal from Fluka, and tetradecanoic acid, tetradecanol, hexadecanol, and hexadecanoic acid from Sigma. Hexa-, hepta-, and octadecanal were synthesized from the alcohols by using the 2-iodoxy benzoic acid oxidation method in a dimethyl sulfoxide/$CHCL_3$ 1:1 mixture as previously described (Frigerio and Santagostino 1994; Frigerio et al. 1999). All reactions were carried out under an argon atmosphere in oven-dried glassware with magnetic stirring. Solvents used for extraction and purification were distilled prior to use. Nuclear magnetic resonance (NMR) spectra were recorded at 300 (75) MHz on a Varian $^{Unity}$Inova spectrometer with $CDCl_3$ ($\delta$ = 7.26 ppm in $^{1}$H NMR spectra and $\delta$ = 77.0 ppm in $^{13}$C NMR spectra) as internal standards and analyzed by SpinWorks3.1.8 (copyright 2011, Kirk Marat, University of Manitoba, Winnipeg, Canada). NMR spectra are available on request from the authors. Gas chromatography using an Agilent GC 6890N (Agilent Technologies) revealed a purity between 98% and 95%.

### Odor exposure

#### *Odor exposure for OB analyses*

For the exposure to an odor, adult mice (2–12 months old) were placed individually into a clear closed plastic box (ca. 10 cm height × 13 cm width × 20 cm length), which had 2 connections to attach plastic tubes (10 cm length, 0.8 cm inner diameter) on one side and small holes for the outgoing air on the opposite side. The box was supplied with a constant stream of air (4 L/min) flowing through an activated charcoal filter and a manual 3-way valve. The valve was adjusted to deliver into the box either a stream of air through 1 tube or air containing an odorant through the other tube. Prior to the exposure to the odorant, the mice were exposed to air for 60 min for the detection of c-fos mRNA or 120 min for the detection of c-Fos protein; this allowed the animals to acclimate to the box and to decrease c-fos level due to cage and self-odors. In the meantime, the test substance (~25 mg) was placed into 1 of the 10 cm tubes and prewarmed to 37 °C allowing material to evaporate. Charcoal-filtered air flowing over this material was passed into the box. The mice were exposed to the odorant in intervals to minimize adaptation. The odorant was presented for 2 min, then air for 3 min; 6 such intervals were performed within 30 min. After this stimulus period, the mice were either sacrificed immediately for in situ hybridization analyses or after 60 min for immunohistochemistry.

#### *Odor exposure for OE analyses*

For the exposure to an odor, young mice (postnatal day, P13–P15) were placed individually into a closed plastic box (ca. 6 cm height × 10 cm width × 10 cm length). Prior to the exposure to the odorant, the mice were kept in the box for 120 min; in the meantime, the test substance (~25 mg) was placed into a second plastic box of the same size. The animals were transferred into this box for 60 min. After exposure to the odor, they were put back to the first box for 30 min and then killed by $CO_2$.

### Immunohistochemistry

For sectioning, all bones surrounding the OB and the nasal turbinates were excised. To remove the air from the nasal cavity, the specimens were immersed in fixative (4% paraformaldehyde in 150 mM phosphate buffer, pH 7.4, 4 °C), and a light vacuum was applied for 5 min; fixation was continued for 10 min on ice. Subsequently, the tissue was cryoprotected by incubation in 25% sucrose in phosphate-buffered saline (PBS) (0.85% NaCl, 1.4 mM $KH_2PO_4$, 8 mM $Na_2HPO_4$, pH 7.4) overnight at 4 °C. Finally, the tissue was embedded in ''Tissue Freezing Medium'' (Leica Microsystems) and frozen on dry ice. Twelve micrometer sections were generated using a CM3050S cryostat (Leica Microsystems) and mounted onto microscope slides (Superfrost slides, Menzel). Sections were air dried for 30 min and rinsed in PBS for

10 min at room temperature. Mouse anti-beta-galactosidase (Promega) (1:700) and rabbit anti-c-fos (Santa Cruz Biotechnology) (1:450) were diluted in PBS/0.3% Triton X-100 containing 10% normal goat serum (NGS) (Dianova) and incubated overnight at 4 °C. After 3 rinses for 5 min in PBS, the bound primary antibodies were visualized by incubating appropriate secondary antibodies conjugated to Alexa 488 or Alexa 568 (Invitrogen) diluted in PBS/0.3% Triton X-100 containing 10% NGS for 2 h at room temperature. After washing for 3 times for 5 min, the sections were counterstained with 4′,6-Diamidin-2′-phenylindoldihydrochlorid (DAPI) (1 μg/mL, Sigma Aldrich) for 3 min at room temperature, rinsed with $H_2O$, and mounted in MOWIOL (33% glycerin, 13% polyvinylalcohol 4-88 [Sigma] in 0.13 M Tris pH 8.5).

### In situ hybridization

A digoxigenin-labeled antisense riboprobe for c-fos (NCBI accession number NM_010234) was generated from a partial cDNA clone (positions 160–1841) in pGem-T vector by using the T7/SP6 RNA transcription system (Roche Diagnostics) as recommended by the manufacturer. In situ hybridization experiments were performed on 12-μm section that were prepared from unfixed tissue embedded in Tissue Freezing Medium and frozen on dry ice. Sections were adhered to starfrost slides (Knittel Gläser) and fixed with 4% paraformaldehyde in 0.1 M $NaHCO_3$, pH 9.5 for 45 min at 4 °C. They were incubated in PBS for 1 min, 0.2 M HCl for 10 min, 1% Triton X-100 for 2 min, and finally twice in PBS for 30 s, all at room temperature. Subsequently, the sections were incubated in 50% formamide in 5× standard sodium citrate (SSC) (1× SSC: 150 mM NaCl, 15 mM Na-citrate, pH 7.0) for 10 min. The sections were then covered with hybridization buffer (50% formamide, 2× SSC, 10% dextran sulfate, 0.2 mg/mL yeast tRNA, 0.2 mg/mL sonicated herring sperm DNA) containing the probe and incubated in a humid chamber (50% formamide) at 65 °C overnight. For posthybridization, the sections were washed twice for 30 min in 0.1× SSC at 65 °C and treated with 1% blocking reagent (Roche Diagnostics) in Tris-buffered saline (TBS) (100 mM Tris, pH 7.5, 150 mM NaCl) with 0.3% Triton X-100 for 30 min at room temperature. They were then incubated with an anti-digoxigenin alkaline phosphatase (AP)–conjugated antibody (Roche Diagnostics) diluted 1:750 in 1% blocking reagent in TBS with 0.3% Triton X-100 for 30 min at 37 °C. After 2 washes in TBS for 10 min, they were rinsed in AP buffer (100 mM Tris, pH 9.5, 100 mM NaCl, 50 mM $MgCl_2$). Hybridization signals were visualized by using nitroblue tetrazolium and 5-bromo-4-chloro-3-indolyl phosphate in AP buffer as substrates. Finally, the sections were rinsed with $H_2O$ and mounted in MOWIOL.

### X-Gal staining

For detecting β-galactosidase activity, freshly frozen tissue was sectioned and mounted onto starfrost slides (Knittel Gläser). The sections were fixed with 0.5% glutaraldehyde in PBS for 10 min at 4 °C, rinsed with $H_2O$, and incubated with buffer A (100 mM phosphate buffer pH 7.4, 1 mM $MgCl_2$, and 5 mM ethyleneglycol-bis(2-aminoethylether)-*N*,*N*,*N*′,*N*′-tetraacetic acid) followed by incubation in buffer B (100 mM phosphate buffer pH 7.4, 1 mM $MgCl_2$, 0.01% sodium deoxycholate, and 0.02% Nonidet P40), each for 5 min at room temperature. The blue precipitate was generated by exposure in the dark at 37 °C to buffer C (buffer B with 5 mM potassium ferricyanide, 5 mM potassium ferrocyanide, and 1 mg/mL of X-Gal) for 1–3 h. Sections were finally washed in distilled water, optionally incubated for 2 min with toluidine blue solution (0.1% toluidine blue, SERVA, in 10% acetic acid), washed again with distilled water, dried, and mounted in Vectamount mounting medium (Vector Laboratories).

### Microscopy and photography

Sections were analyzed using a Zeiss Axiophot microscope (Carl Zeiss MicroImaging). Images were captured using a Zeiss Axiocam for transmitted light and a "Sensi-Cam" CCD camera (PCO-imaging) for fluorescent images.

### Quantitative analyses

Quantitative analyses were performed according to Oliva et al. (2008). For cell counts, the sections were examined with a ×40 objective. An OR37 glomerulus was defined as a region of X-gal or green fluorescent protein–labeled neuropil delimited by toluidine blue or DAPI-stained juxtaglomerular cells (JCs); c-Fos immunoreactive and DAPI-stained cells that were immediately adjacent to the OR37 glomerulus (maximal 4 nuclei widths from the outer boundary of the axon fibers within the glomerulus) were counted in serial sections. c-Fos signals were counted when their signal intensity was above background and the signal was colocalized with a DAPI-stained nucleus. The percentage of c-Fos immunoreactive cells from the number of DAPI-stained cells surrounding the glomeruli was determined and given as means ± standard error of the mean. Statistical significances were determined by an unpaired *t*-test using the Graphpad software (GraphPad Software, Inc.); these values were corrected by Bonferroni correction. For comparing the different aldehydes, the significance was therefore set at $P < 0.003$ ($\alpha = 0.05$, pairwise comparisons = 15); for comparing the aldehydes with alcohols and acids, the significance was set at $P < 0.016$ ($\alpha = 0.05$, pairwise comparisons = 3).

### Immunocytochemistry

The olfr62 and OR37A were expressed as N-terminal fusion proteins with the first 39 amino acids of bovine rhodopsin in a modified pcDNA5/FRT/TO (Invitrogen) vector. The pRK5-Rho expression vector containing the rho-tagged IC6 receptor was kindly provided by Dietmar Krautwurst (Deutsche Forschungsanstalt für Lebensmittelchemie,

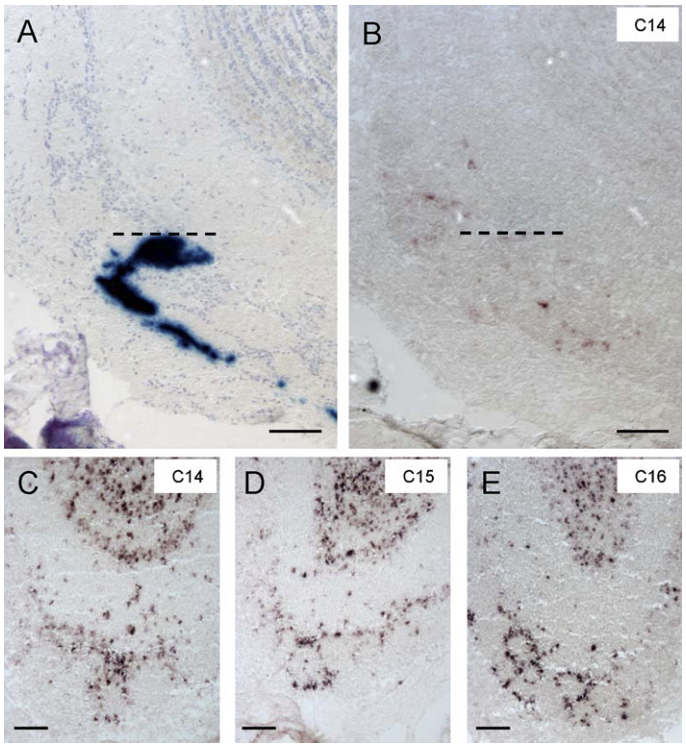


**Figure 1** Exposure of mice to long-chain hydrocarbons activates glomeruli in the OR37 area of the mouse OB. (**A**) X-Gal–stained section through the OR37A glomerulus counterstained with toluidine blue. (**B**) Adjacent section to the one shown in A hybridized with a c-fos–specific antisense riboprobe; after exposure of the mouse to tetradecane (C14), the OR37A glomerulus is not surrounded by c-fos–reactive cells. The dotted line indicates the position of the OR37A glomerulus. (**C**) Section from the neighborhood of the OR37A glomerulus; after exposure of the mouse to tetradecane, c-fos–positive glomeruli are visible in the ventral domain of the bulb. (**D**) Cross section through the OR37 area of the bulb; after exposure of the mouse to pentadecane (C15), c-fos–positive glomeruli are visible in the ventral domain of the bulb. (**E**) Cross section through the OR37 area of the bulb; after exposure of the mouse to hexadecane (C16), c-fos–positive glomeruli are visible in the ventral domain of the bulb. Scale bars, A–E: 100 μm. This figure appears in color in the online version of *Chemical Senses*.

TU-München). Receptor expression was monitored 24 h posttransfection. Cells were fixed for 4 min in 4% methanol-free paraformaldehyde (Polyscience Inc.) and permeabilized with 0.25% Triton X-100 for 4 min. To monitor cell surface expression, the permeabilization step was omitted. All solutions were diluted in PBS. Subsequently, unspecific binding was blocked with 5% fetal calf serum for 30 min. Cells were incubated in a 1:500 dilution overnight with a primary monoclonal mouse IgG B6-30 directed against the N-terminal rhodopsin epitope kindly provided by W. Clay Smith (University of Florida). Fluorescence labeling was obtained by 1-h incubation with a 1:2000 dilution of a polyclonal goat anti-mouse Alexa Fluor 546–conjugated secondary antibody (Invitrogen). Counterstaining of the cell nuclei was achieved with Hoechst 33342 at 1:10 000 dilution. For analysis, we used the fully automated high content imaging system BD Pathway Bioimager 855 (BD Bioscience).

### Cell culture

Cell culture was essentially performed as described in Bufe et al. (2002). Briefly, HEK293T cells were grown in cell culture medium DMEM (Sigma), containing 5% heat inactivated bovine calf serum (Biochrom), 10 000 U/mL penicillin G (Sigma), 10 mg/mL streptomycin (Sigma), and 2 mM L-glutamine (Sigma). Cells were cultured till 80–90% confluence and seeded in 1:10 dilutions on optic 96-well μ-clear plates (Greiner) coated with 10 μg/mL poly-D-lysine (Sigma). After 24 h, cells were cotransfected with a given OR, the G-protein chimera G15-Golf47 and RTP1s in equal amounts using jetPEI (PeqLab).

### Calcium imaging

For single-cell calcium imaging with the Bioimager, cells were incubated 24–48 h posttransfection with bath solution containing 2 μM Fura 2 AM (Invitrogen), 1.25 mM probenecid, and 5% signal enhancer from the ratiometric calcium assay kit (BD Bioscience) for 2 h. Changes in calcium-dependent fluorescence were recorded with the Bioimager at 0.5 Hz data acquisition rate and analyzed using the attovision 1.6 software (BD Bioscience).

FLIPR experiments were performed essentially as described in Bufe et al. (2002). Briefly, HEK293T cells were incubated 24–48 h posttransfection with bath solution containing 2 μM Fluo 4 AM (Invitrogen) and 1.25 mM probenecid for 2 h. Changes in calcium-dependent fluorescence were recorded with the FLIPR3 at 0.5 Hz data acquisition rate and analyzed using the FLIPR 2.1.2 software (Molecular Devices).

## Results

A first straightforward approach to assess whether long-chain hydrocarbons may be recognized by OR37 receptors, analyzing the activity of the corresponding glomeruli in the OB by live imaging techniques, as performed for glomeruli at the dorsal and lateral surface (Meister and Bonhoeffer 2001; Fried et al. 2002; Spors and Grinvald 2002; Wachowiak and Cohen 2003; Mizrahi et al. 2004; Takahashi et al. 2004; Igarashi and Mori 2005; Lin et al. 2006; McGann et al. 2006; Oka et al. 2006; Fletcher et al. 2009), was not practicable because the OR37 glomeruli are located on the ventral surface of the OB and therefore not accessible for such imaging approaches. As an alternative, we decided to use the expression of the immediate early gene c-fos in JCs as an indicator of glomerular activation; this procedure has been successfully applied in several recent studies (Guthrie et al. 1993; Lin et al. 2004; Salcedo et al. 2005; Oliva et al. 2008; Clarin et al. 2010). Our transgenic mouse lines in which the glomeruli for 3 distinct OR37 subtypes can be visualized by axonal markers (Strotmann et al. 2000) allow to unequivocally identify the distinct OR37

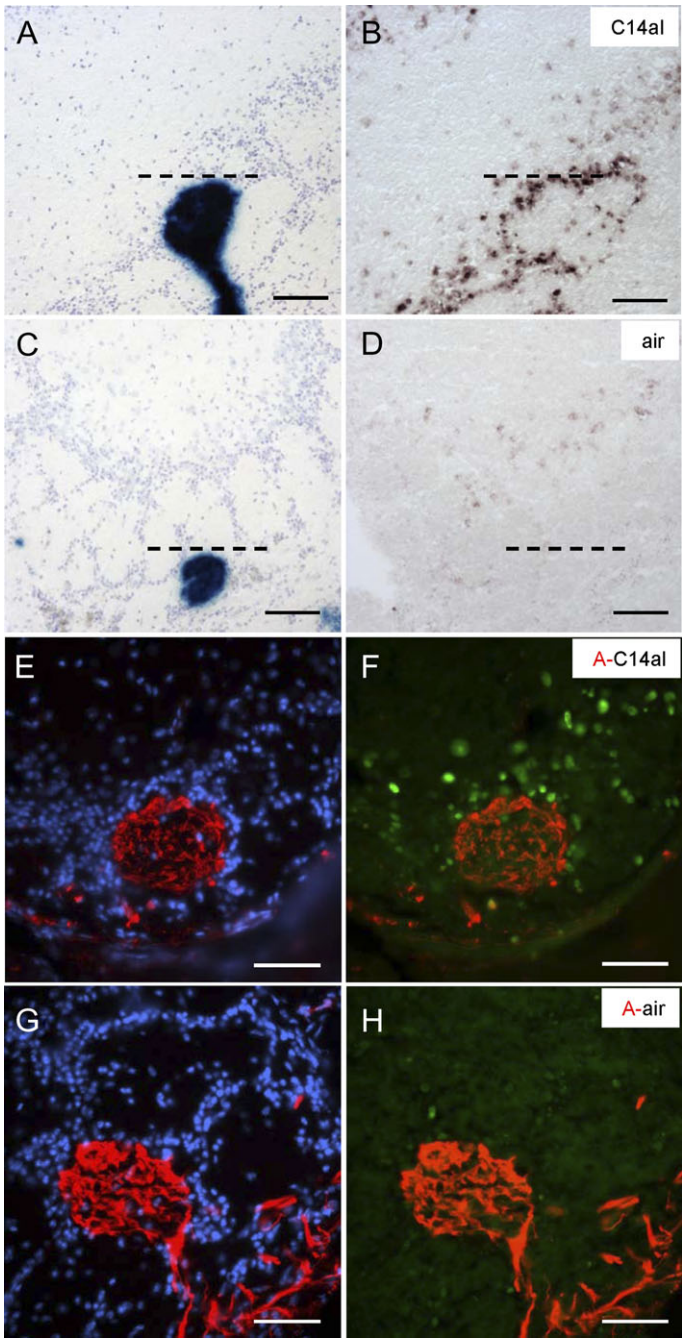


**Figure 2** The OR37A glomerulus is activated after exposure of the mouse to tetradecanal. (**A**) X-Gal–stained section through the OR37A glomerulus counterstained with toluidine blue. The dotted line indicates the position of the OR37A glomerulus. (**B**) Adjacent section to A hybridized with an antisense riboprobe to c-fos; after exposure of the mouse to tetradecanal (C14al), the OR37A glomerulus is encircled by numerous positive cells. The dotted line indicates the position of the OR37A glomerulus. (**C**) X-Gal–stained section through the OR37A glomerulus counterstained with toluidine blue. (**D**) Adjacent section to C hybridized with an antisense riboprobe to c-fos; after exposure of the mouse to clean air, no c-fos–positive cells are detectable at the OR37A glomerulus. The dotted line indicates the position of the OR37A glomerulus. (**E**) Cross section through the OR37A glomerulus which is visualized with an antibody against β-galactosidase; the section is counterstained with DAPI. (**F**) The OR37A glomerulus is encircled by numerous cells containing the c-Fos protein after exposure of the mouse to tetradecanal. (**G**) Cross section through the OR37A glomerulus which is visualized by an antibody against β-galactosidase; counterstaining with DAPI. (**H**) After exposure of the mouse to clean air, hardly any c-Fos–positive cells are detectable at the OR37A glomerulus. Scale bars: 100 μm in A to D; 50 μm in E–H. This figure appears in color in the online version of *Chemical Senses*.

glomeruli. In a first set of experiments, the OR37 area was investigated after exposure of mice to the C14 alkane (tetradecane) using the labeled OR37A glomerulus as landmark. On a continuous series of sections through the anterior region of the OB, the OR37A glomerulus could be clearly identified by X-gal staining in the ventral domain, as shown representatively in Figure 1A. Probing adjacent sections with a c-fos–specific antisense riboprobe resulted in hardly any c-fos–positive cells in the proximity of the OR37A glomerulus (Figure 1B). However, inspection of the OR37A neighborhood revealed that glomeruli in this region were encircled by c-fos–positive cells (Figure 1C). This finding is in line with the observation that ventral glomeruli were activated by tetradecane in the rat OB (Ho et al. 2006). Visualizing the glomerulus of another OR37 subtype (OR37B and OR37C) revealed that also these glomeruli were located distantly from the clearly c-fos–positive glomeruli (data not shown). The exposure of mice to the C15 (pentadecane) or the C16 (hexadecane) alkane (Figure 1D,E) resulted in similar patterns of activated glomeruli in the ventral OB; again, neither the OR37A nor the -B or the -C glomerulus was surrounded by significant numbers of c-fos–positive cells (data not shown).

Based on the results that an exposure of mice to the long-chain alkanes elicited activation of glomeruli in a region close to the area of identifiable OR37 glomeruli, we considered structurally related compounds as candidates for activating OR37 glomeruli. Therefore, long-chain compounds with a distinct functional group were assessed next; in first approaches, C14–C16 aldehydes were analyzed. After exposure of mice to tetradecanal, the OR37A glomerulus (Figure 2A) was in fact surrounded by numerous c-fos–positive cells, as shown on a representative section in Figure 2B. In animals, which were exposed to clean air, only very few c-fos–positive cells could be detected at the OR37A glomerulus (Figure 2C,D). Thus, tetradecanal was the first compound that induced activity at the OR37A glomerulus. To obtain a more precise affiliation of the activated cells to this glomerulus, we tried to visualize the c-Fos protein in JCs together with the beta-galactosidase inside the glomerulus by double immunostaining. As shown by a representative section in Figure 2E,F, indeed many cells containing c-Fos protein were visible surrounding the OR37A glomerulus after exposure of mice to tetradecanal, confirming that the C14 aldehyde induced activity at the OR37A glomerulus. Again, as demonstrated for the in situ hybridization, when mice were exposed to clean air, only very few c-Fos protein–positive JCs were detectable at the OR37A glomerulus (Figure 2G,H). The finding that the C14 alkane induced hardly any c-fos expression, but the corresponding C14

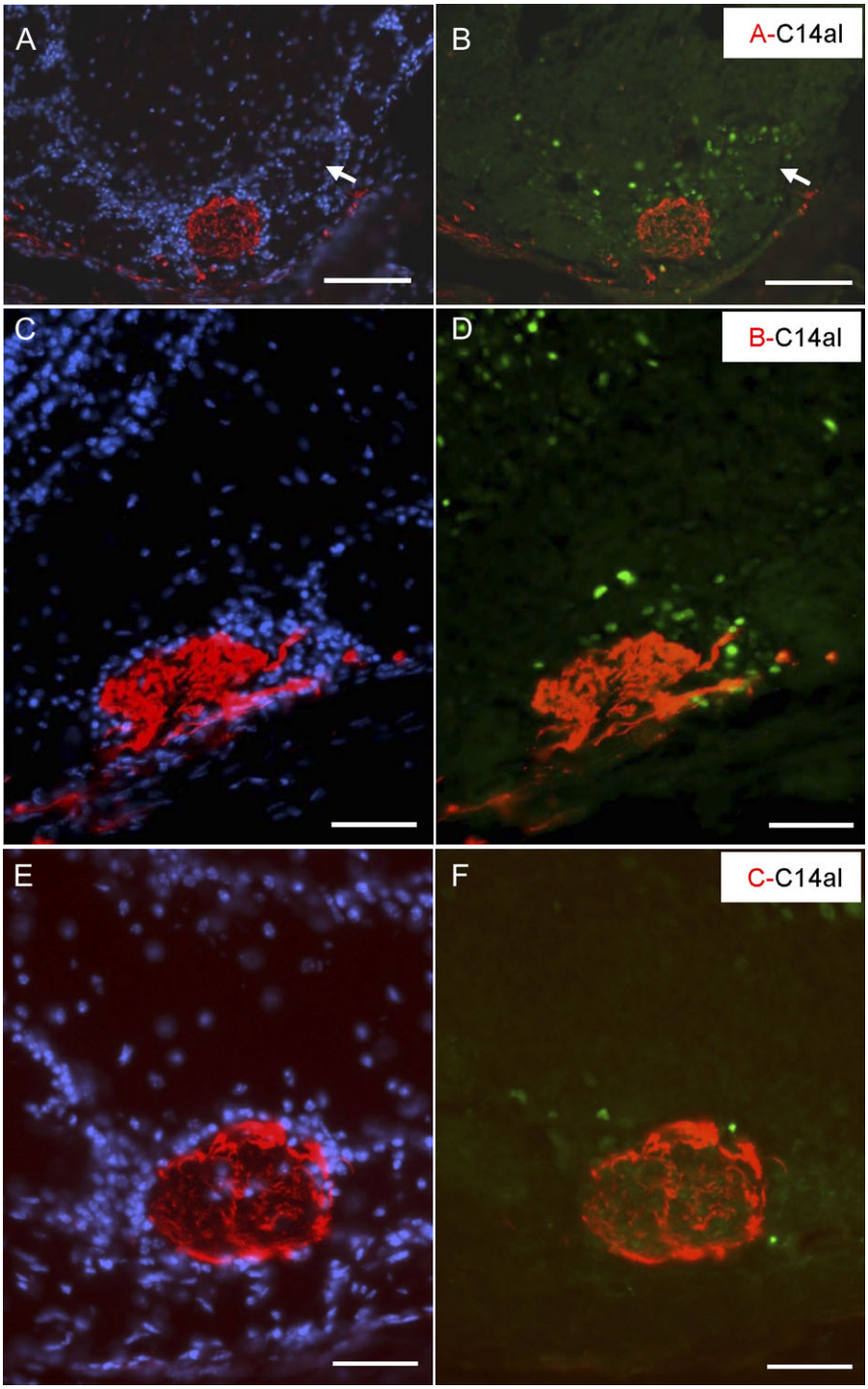


**Figure 3** Tetradecanal activates distinct OR37 glomeruli to a different degree. (**A**) Cross section through the OR37A glomerulus which is visualized with an antibody against β-galactosidase, counterstaining with DAPI. (**B**) After exposure of the mouse to tetradecanal, c-Fos–positive cells are visible at the OR37A glomerulus and neighboring glomeruli (arrow). (**C**) Cross section through the OR37B glomerulus visualized with an antibody against β-galactosidase; counterstaining with DAPI. (**D**) A few c-Fos–positive cells are detectable at the OR37B glomerulus after exposure of the mouse to tetradecanal. (**E**) Cross section through the OR37C glomerulus visualized with an antibody against β-galactosidase, counterstaining with DAPI. (**F**) Hardly any c-Fos–positive cells are detectable at the OR37C glomerulus after exposure of the mouse to tetradecanal. Scale bars: 100 μm in A and B; 50 μm in C–F. This figure appears in color in the online version of *Chemical Senses*.

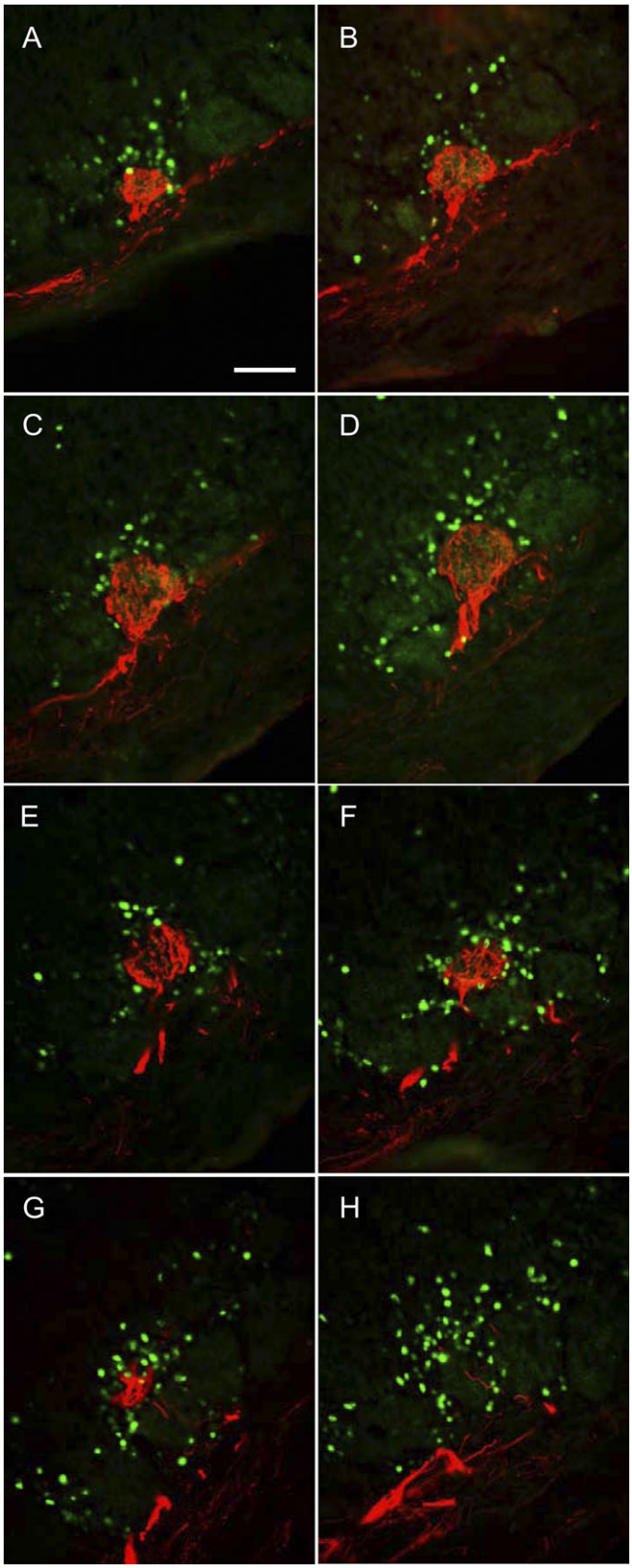


aldehyde was very effective, indicated a significant degree of discrimination capacity of this OR37 subtype.

A closer examination of the sections after the exposure of mice to tetradecanal revealed that several glomeruli in the vicinity of OR37A were also surrounded by c-Fos–positive JCs (Figure 3A,B). The location of these glomeruli close to OR37A raised the possibility that they represent glomeruli formed by the neurons expressing other OR37 subfamily members. To test this, we next analyzed mice in which the OR37B or the OR37C glomerulus, respectively, can be visualized. As shown in Figure 3C,D, the OR37B glomerulus was indeed surrounded by c-Fos–positive cells, indicating its activation by tetradecanal. The lower abundance of positive cells around OR37B suggested that it was less strongly activated than OR37A. Interestingly, hardly any c-Fos–positive cells were visible around the OR37C glomerulus (Figure 3E,F). These results indicated that tetradecanal activated these 3 OR37 glomeruli to a different degree. To obtain a quantitative measure of this observation, we determined the number of c-Fos–positive JCs surrounding the respective glomeruli. For this purpose, a series of sections covering the entire size of a glomerulus, as shown for OR37A in Figure 4, were analyzed. Because glomeruli vary slightly in size and may thus be encircled by different numbers of cells, we also counted the total number of JCs on DAPI-counterstained sections and calculated the percentage of c-Fos–positive cells. It was found that an exposure to tetradecanal elicited c-Fos expression in about 39% (38.7 ± 4.6%; $n$ = 11; Figure 5A) of the JCs at the OR37A glomerulus, in about 16% (16.3 ± 12.1%; $n$ = 7; Figure 5A) at the OR37B glomerulus and about 6% (6.3 ± 3.5%; $n$ = 12; Figure 5A) at the OR37C glomerulus. The number of c-Fos–positive cells surrounding the OR37C glomerulus was not higher than in control animals, which were exposed to clean air (8.1 ± 2.4%; $n$ = 4; Figure 5A). The quantifications confirmed the notion that these OR37 glomeruli responded differentially to tetradecanal.

We next analyzed whether aldehydes with longer chain length induce c-Fos expression in JCs at these glomeruli. The exposure of mice to pentadecanal indeed activated the OR37A glomerulus (Figure 5C,D); in fact, 51.0 ± 7.6% ($n$ = 8) of the JCs were c-Fos positive (Figure 5B), which is significantly more than after exposure to tetradecanal (see Figure 6A). At the OR37B glomerulus, about 46% (46.4 ± 5.6%, $n$ = 5; Figure 5B) of the JCs were c-Fos positive, at the OR37C glomerulus again hardly any cell (5.9 ± 3.8%; $n$ = 8; Figure 5B), comparable to exposure to clean air (8.1 ± 2.4%; $n$ = 4; Figure 5B). Because the increase in chain length resulted in fewer activated JCs around OR37A, but more around OR37B, even longer aldehydes were analyzed

**Figure 4** Series of sections through the OR37A glomerulus of a mouse exposed to tetradecanal; on every section, numerous c-Fos–positive cells surrounding this glomerulus are detectable. Scale bar: 50 μm in A–H. This figure appears in color in the online version of *Chemical Senses*.

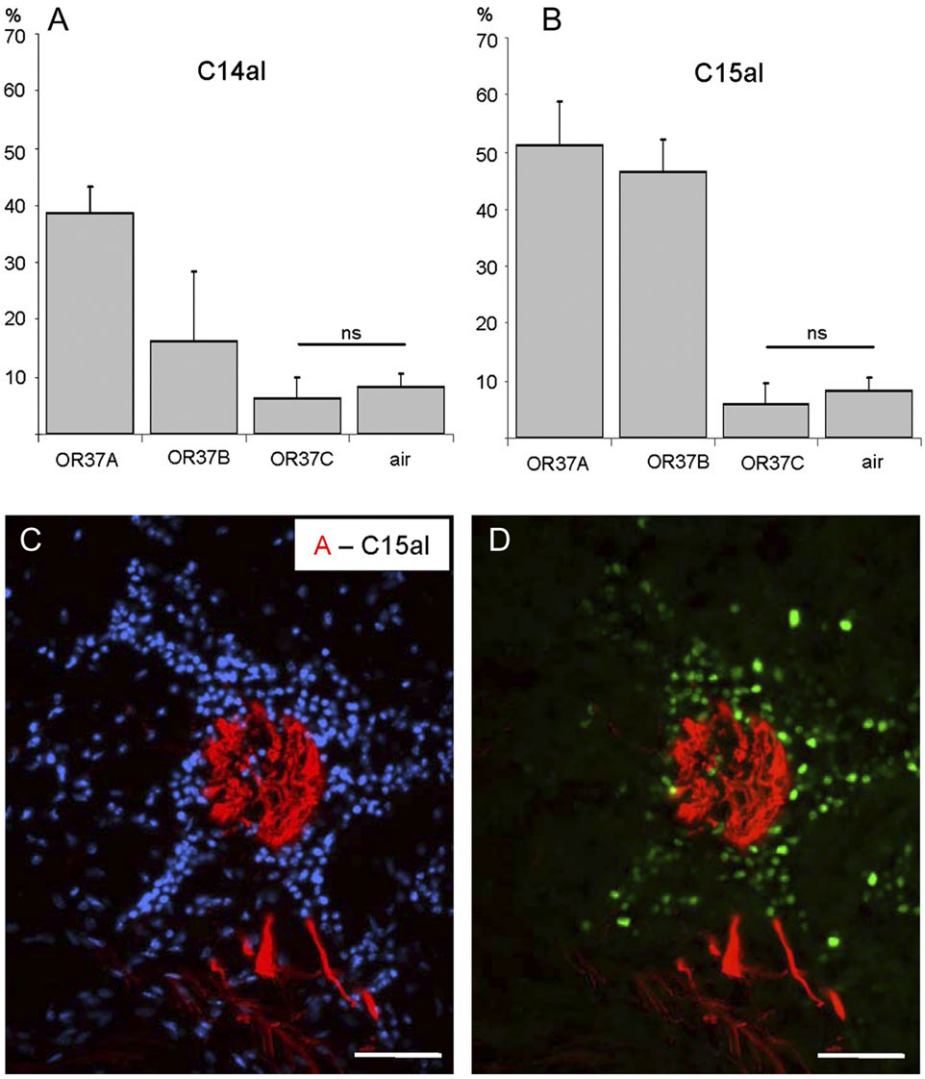


**Figure 5** Differential activation of the OR37A, B, and C glomeruli after exposure of mice to long-chain aldehydes. (**A**) Percentage of c-Fos–positive JCs induced by tetradecanal (C14al) compared with clean air exposure. Tetradecanal: OR37A: 38.7 ± 4.6% ($n$ = 11); OR37B: 16.3 ± 12.1% ($n$ = 7); OR37C: 6.3 ± 3.5% ($n$ = 12). Clean air: OR37C: 8.1 ± 2.4% ($n$ = 4). ns, statistically not significant. (**B**) Percentage of c-Fos–positive JCs induced by pentadecanal (C15al) compared with clean air exposure. Pentadecanal: OR37A: 51.1 ± 7.7% ($n$ = 8); OR37B: 46.4 ± 5.6% ($n$ = 5); OR37C: 5.9 ± 3.8% ($n$ = 8). Clean air: OR37C: 8.1 ± 2.4% ($n$ = 4). ns, statistically not significant. (**C**) Cross section through the OR37A glomerulus visualized by an antibody against β-galactosidase, counterstaining with DAPI. (**D**) After exposure of the mouse to pentadecanal (C15al), the OR37A glomerulus is encircled by c-Fos–positive cells. Scale bar: 50 μm in C and D. This figure appears in color in the online version of *Chemical Senses*.

next. At the OR37A glomerulus, the number of c-Fos–positive cells decreased when the chain length was increased from C16 to C18; the C17 and C18 aldehydes were not different from the air control (Figure 6A). At the OR37B glomerulus, the number of activated JCs was increasing from the C14 to C16 aldehyde and decreased from C16 to C18 (Figure 6B). Interestingly, at the OR37C glomerulus, a large number of c-Fos–positive cells were detectable for the C16 and C17 aldehydes; the number decreased again from C17 to C18 (Figure 6C). Together, these results indicated that the glomeruli of 3 highly homologous members of the OR37 subfamily were differentially activated upon exposure of mice to a particular long-chain fatty aldehyde (multiple statistical comparison of glomerular activation is shown in Supplementary Table 1). To directly visualize this feature in one individual, we crossed the transgenic lines in which the OSNs with different OR37 subtypes coexpress distinct histological markers (Strotmann et al. 2000) and exposed them to selected aldehydes. In the OB of OR37A/C double transgenic mice, tetradecanal induced c-Fos expression in many cells surrounding the OR37A glomerulus (Figure 7A), whereas the OR37C (Figure 7B) glomerulus was almost devoid of labeled cells. A similar result was obtained after exposure of OR37B/C double transgenic mice to pentadecanal: in this case, the OR37B glomerulus (Figure 7D) was intensely labeled and the OR37C glomerulus (Figure 7E) was

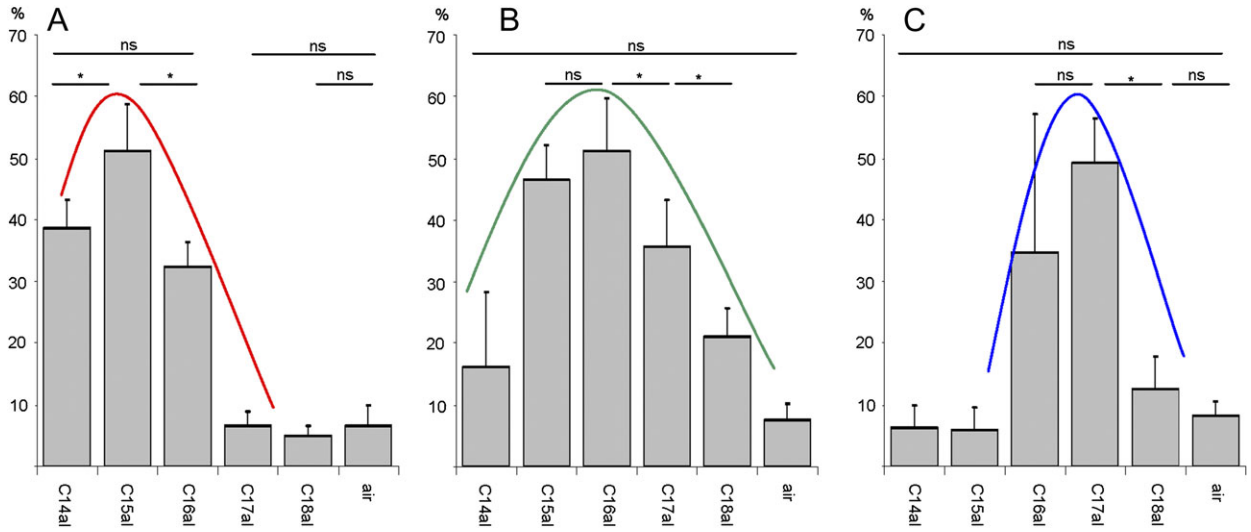


**Figure 6** Differential activation of the OR37A, -B, and -C glomeruli after exposure of mice to long-chain aldehydes. (**A**) Percentage of c-Fos–positive JCs at the OR37A glomerulus induced by long-chain aldehydes. C14al: 38.7 ± 4.6% ($n$ = 11); C15al: 51.0 ± 7.6% ($n$ = 8); C16al: 32.3 ± 4% ($n$ = 6); C17al: 6.5 ± 2.6% ($n$ = 8); C18al: 4.9 ± 1.8% ($n$ = 7); clean air: 6.6 ± 3.3% ($n$ = 6). The curve illustrates the response profile of the OR37A glomerulus toward C14–C18 aldehydes. *, statistically significant; ns, statistically not significant. (**B**) Percentage of c-Fos–positive JCs at the OR37B glomerulus induced by long-chain aldehydes. C14al: 16.3 ± 12.1% ($n$ = 7); C15al: 46.4 ± 5.6% ($n$ = 5); C16al: 51.2 ± 8.8% ($n$ = 12); C17al: 35.7 ± 7.7% ($n$ = 6); C18al: 21.1 ± 4.8% ($n$ = 7); clean air: 7.7 ± 2.7% ($n$ = 8). The curve illustrates the response profile of the OR37B glomerulus toward C14–C18 aldehydes. *, statistically significant; ns, statistically not significant. (**C**) Percentage of c-Fos–positive JCs at the OR37C glomerulus induced by long-chain aldehydes. C14al: 6.3 ± 3.5% ($n$ = 12); C15al: 5.9 ± 3.8% ($n$ = 8); C16al: 34.8 ± 22.4% ($n$ = 6); C17al: 49.1 ± 7.3% ($n$ = 9); C18al: 12.5 ± 5.5% ($n$ = 9); clean air: 8.1 ± 2.4% ($n$ = 4). The curve illustrates the response profile of the OR37C glomerulus toward C14–C18 aldehydes. *, statistically significant; ns, statistically not significant. This figure appears in color in the online version of *Chemical Senses*.

almost without c-Fos–positive JCs. The results thus confirmed the differential responsiveness of distinct OR37 glomeruli in one individual.

The finding that the glomeruli robustly responded to aldehydes of different chain lengths but were basically unresponsive to the corresponding alkanes suggested rather high ligand specificity. To further explore this feature, we examined the OR37A and the OR37B glomerulus for their responsiveness to carbon compounds with distinct functional groups. For OR37A, the C14 compounds were tested, for OR37B the C16 compounds, because the respective aldehydes induced strong activation at these glomeruli. The exposure to the alcohol compound tetradecanol (Figure 8A,B) or to tetradecanoic acid (Figure 8C,D) induced expression of c-Fos in significantly fewer cells around the OR37A glomerulus than the aldehyde (tetradecanal vs. tetradecanol: 38.7 ± 4.6% vs. 26.0 ± 5.9%; $n$ = 5 for tetradecanol, $P$ = 0.0004) (tetradecanal vs. tetradecanoic acid: 38.7 ± 4.6% vs. 9.3 ± 3%; $n$ = 6 for tetradecanoic acid, $P$ = 0.0001) (Figure 8G). With the acid compound, a glomerulus next to OR37A was activated in several bulbs (see Figure 8D), in these cases, some c-Fos–positive cells were positioned at the border between these glomeruli, thereby increasing the number of c-Fos–positive cells that were counted around OR37A, which implicated overestimating the amount of activated cells for OR37A. Thus, the OR37A glomerulus showed selectivity for the aldehyde. The exposure of mice to the C16 alcohol (Figure 8F) was significantly less effective in activating the OR37B glomerulus (18.3 ± 6.6%; $n$ = 8) than the aldehyde (Figure 8E); less than half as many JCs were c-Fos positive (Figure 8H). A neighboring glomerulus to OR37B was activated by hexadecanol in several cases (e.g., see Figure 8F), thus also leading to an overrating for this compound at OR37B. An exposure to hexadecanoic acid resulted in even fewer positive cells (4.3 ± 5.5%; $n$ = 9) (Figure 8H). These data showed that also the OR37B glomerulus showed selectivity for the aldehyde.

These analyses revealed that OR37 glomeruli were strongly activated when mice were exposed to long straight chain aldehydes, which are also termed fatty aldehydes. To our knowledge, these molecules have not been described as ligands for other ORs, raising the question, whether they activate other glomeruli, as well. To obtain first insight into this question, the sections containing the OR37 glomeruli were examined for glomeruli with c-Fos–positive JCs. As shown in Figure 9A,B, an exposure of mice to pentadecanal induced c-Fos expression at several glomeruli which were grouped around OR37A within the ventral domain of the bulb. In the medial or lateral domains (Figure 9C,D), glomeruli showed very little c-Fos expression; a few activated glomeruli could be detected also in these domains (data not shown), however, they were sparse. An analysis of the ventral region of the bulb along the anterior–posterior axis revealed that groups of activated glomeruli similar to the one seen in

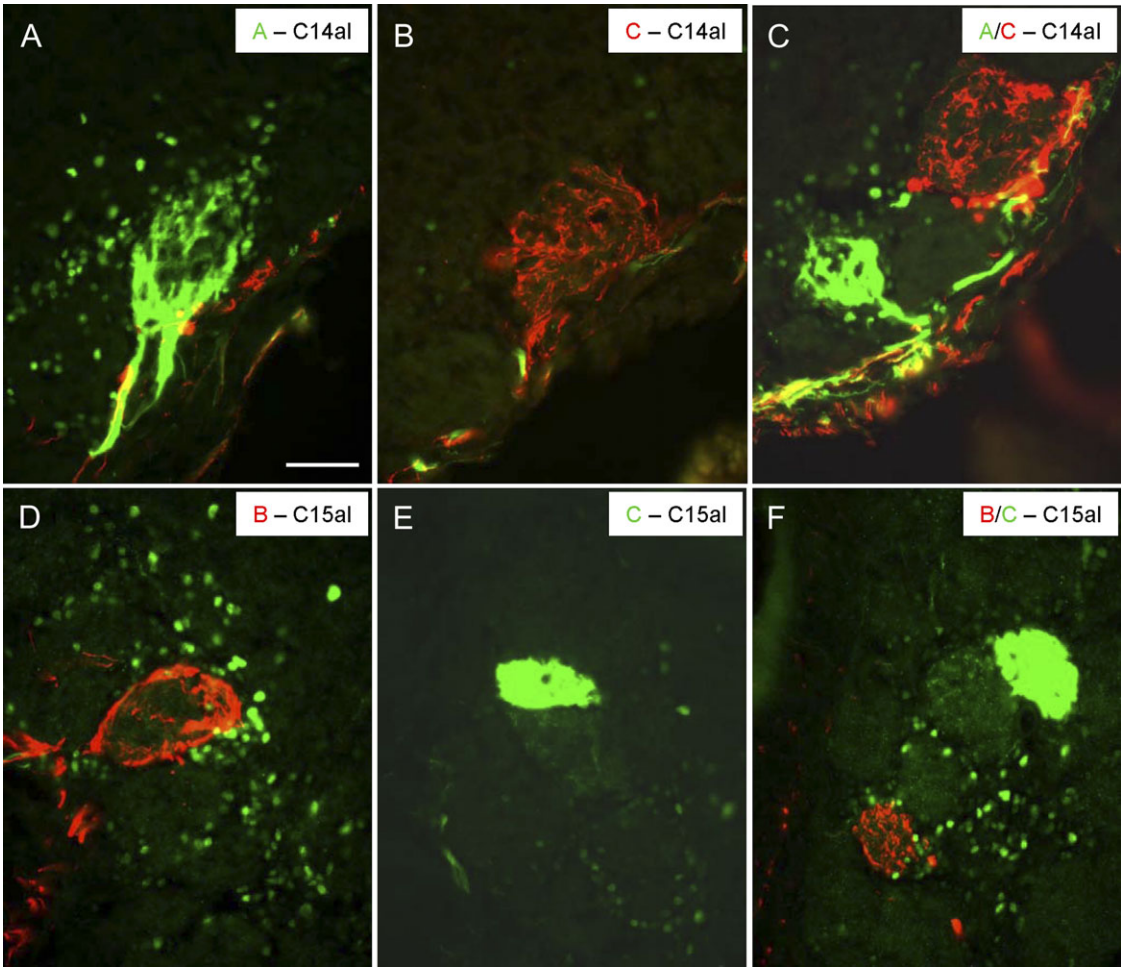


**Figure 7** Long-chain aldehydes activate distinct OR37 glomeruli to a different degree. (**A**) Cross section through the OR37A glomerulus (visualized by intrinsic green fluorescent protein fluorescence) from an OR37A-ITGFP/OR37C-ITlacZ double transgenic mouse. After exposure to tetradecanal, numerous c-Fos–immunoreactive cells (visualized by an anti-c-fos antibody in green) are detectable surrounding the OR37A glomerulus. (**B**) Cross section (84 μm distant from the one shown in A) through the OR37C glomerulus (visualized by an anti-β-galactosidase antibody in red) from the same individual as in A. After exposure to tetradecanal, hardly any c-Fos–positive cells are detectable at the OR37C glomerulus. (**C**) Cross section with a cut through the OR37A (green) and the OR37C glomerulus (red); c-Fos–positive cells (green) are visible at the OR37A glomerulus but not at the OR37C glomerulus after exposure to tetradecanal. (**D**) Cross section through the OR37B glomerulus (visualized by an anti-β-galactosidase antibody in red) from an OR37B-ITlacZ/OR37C-ITGFP double transgenic individual. After exposure to pentadecanal, numerous c-Fos–immunoreactive cells (visualized by an anti-c-fos antibody in green) are visible surrounding the OR37B glomerulus. (**E**) Cross section (48 μm distant from the one shown in D) through the OR37C glomerulus (visualized by intrinsic GFP fluorescence) from the same individual as in D. Hardly any c-Fos–positive cells are detectable at this glomerulus after exposure to pentadecanal. (**F**) Cross section with a cut through the OR37B glomerulus (red) and the OR37C glomerulus (green); c-Fos–positive cells (green) are visible at the OR37B glomerulus but not at the OR37C glomerulus after exposure to pentadecanal. Scale bar: 50 μm in A–F. This figure appears in color in the online version of *Chemical Senses*.

Figure 9B were detectable in the anterior part of the bulb, covering an area of about 600 μm; the OR37 glomeruli were constantly found within that region. Posterior to that domain, hardly any c-Fos–positive glomeruli were detectable, not even in the ventral region (Figure 9E,F). These analyses indicated that pentadecanal induced c-Fos expression predominantly in the anterior–ventral domain of the bulb.

Altogether, these analyses revealed that an exposure of mice to distinct fatty aldehydes induced c-Fos expression in JCs at defined OR37 glomeruli. These data strongly suggested that the OR37 receptors and thus the corresponding sensory neurons, which express these ORs, were activated. To confirm this notion, we first tried to assay a representative OR37 receptor in a heterologous expression system. In an attempt to examine the agonist profile of the OR37A receptor in a heterologous expression system, we applied conditions that were successfully used for the functional characterization of the mouse OR olfr62 (Zhuang and Matsunami 2007). While we could see robust calcium transients for olfr62 upon stimulation with its cognate ligand 2-coumaranone, we observed an activation of OR37A neither by tridecanal, tetradecanal, tetradecanol, and other odorants

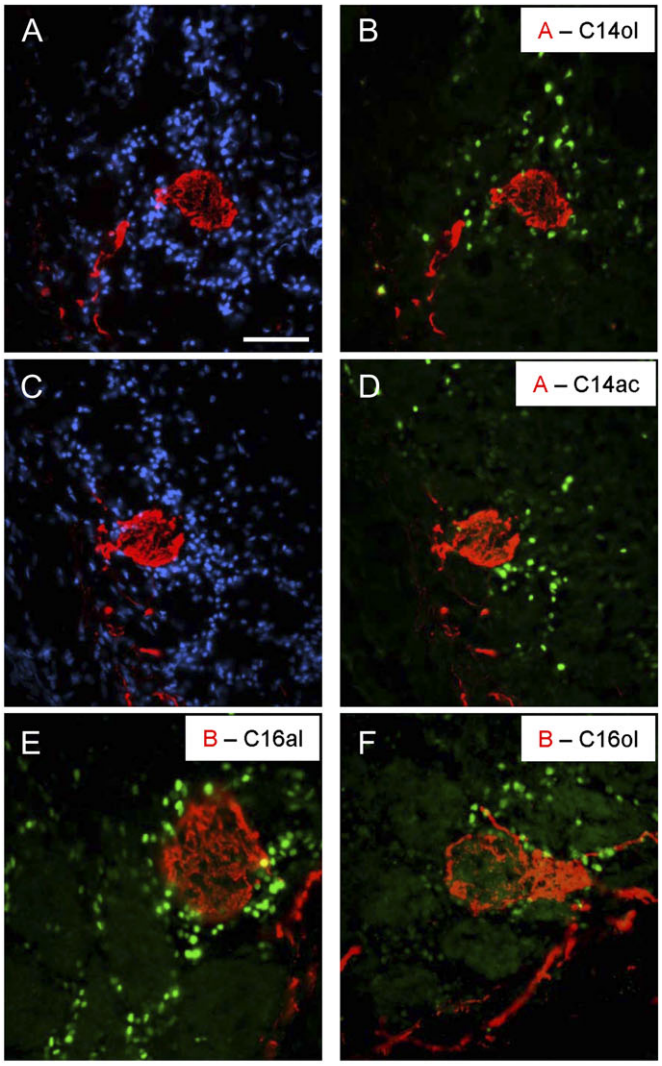


**Figure 8** Compounds with the same carbon chain length but distinct functional groups activate an OR37 glomerulus to a different degree. (**A**) Cross section through the OR37A glomerulus visualized by an antibody against β-galactosidase, counterstaining with DAPI. (**B**) A few c-Fos–positive cells are detectable at the OR37A glomerulus after exposure of the mouse to tetradecanol (C14ol). (**C**) Cross section through the OR37A glomerulus visualized by an antibody against β-galactosidase, counterstaining with DAPI. (**D**) A few c-Fos–positive cells are detectable at the OR37A glomerulus after exposure of the mouse to tetradecanoic acid (C14ac). (**E**) Cross section through an OR37B glomerulus visualized by an antibody against β-galactosidase; numerous c-Fos–positive cells are detectable at the glomerulus after exposure of the mouse to hexadecanal (C16al). (**F**) Cross section through an OR37B glomerulus visualized by an antibody against β-galactosidase; a few c-Fos–positive cells are detectable at the glomerulus after exposure of the mouse to hexadecanol (C16ol). (**G**) Percentage of c-Fos–positive JCs at the OR37A glomerulus after exposure of mice to compounds with the same carbon chain length but distinct functional groups. Tetradecanal: 38.7 ± 4.6% ($n$ = 11); tetradecanol: 26.0 ± 5.9% ($n$ = 5); and tetradecanoic acid: 9.3 ± 3% ($n$ = 6). *, statistically significant. (**H**) Percentage of c-Fos–positive JCs at the OR37B glomerulus after exposure of mice to compounds with the same carbon chain length but distinct functional groups. Hexadecanal: 51.2 ± 8.8% ($n$ = 12); hexadecanol: 18.3 ± 6.6% ($n$ = 8); hexadecanoic acid: 4.3 ± 5.5% ($n$ = 9). *, statistically significant. Scale bar: 50 μm in A–F. This figure appears in color in the online version of *Chemical Senses*.

(Supplementary Figure 1) nor by tridecanol, tetradecanoic acid, and hexadecanal (data not shown). Control experiments showed that the lack of response was not caused by noticeable differences in expression and cell surface localization. However, we saw that other ORs with identified ligands also show only a weak or no detectable response. One possible explanation for the lack of activation of OR37A thus may be that ORs differ in their capability to couple to the chimeric G-protein G15-Golf47.

We therefore analyzed next whether native OSN expressing the OR37 receptors were activated by visualizing c-Fos expression in the OE after exposure of mice to selected compounds. On cross sections through the OE of transgenic animals, OSNs expressing a defined OR37 subtype were identified using immunohistochemical detection of β-galactosidase, as shown for OR37A in Figure 10A. An exposure of mice to pentadecanal, which strongly activated the OR37A glomerulus, induced expression of c-Fos in distinct cells in the OSN layer (Figure 10B); a punctuate labeling was obtained, consistent with the location of the c-Fos protein in the nucleus. An overlay of the c-Fos staining and the OR37A immunoreactivity revealed that OR37A expressing OSNs were c-Fos positive, demonstrating that they were indeed activated (Figure 10C). Using pentadecane—which induced no c-Fos expression around the OR37A glomerulus—as a stimulus, led to c-Fos expression in the OE (Figure 10E), however, OSNs expressing OR37A were not positive (Figure 10F). To verify that heptadecanal, which strongly activated the OR37C glomerulus, accordingly activated the OR37C expressing cells, corresponding experiments were performed using mice from this line. As seen in Figure 10G–I, these cells were in fact c-Fos positive.

## Discussion

In the present study, we have demonstrated that an exposure of mice to an airstream containing long-chain aliphatic compounds induced the expression of c-fos in JCs surrounding distinct glomeruli. These findings demonstrate that the

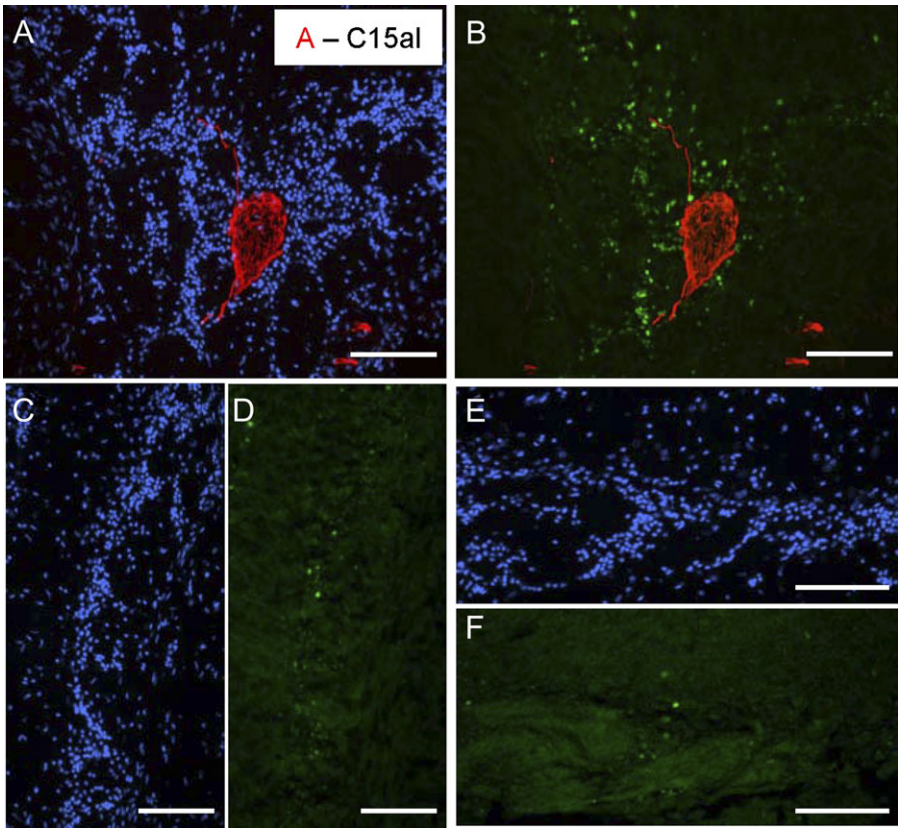


**Figure 9** Distribution of activated glomeruli after stimulation with a long-chain fatty aldehyde. (**A**) Cross section through the anterior–ventral region of the bulb counterstained with DAPI. The OR37A glomerulus is visualized by an antibody against β-galactosidase. (**B**) After exposure of the mouse to pentadecanal (C15al), clusters of glomeruli in the ventral domain are surrounded by numerous c-Fos–positive cells. The OR37A glomerulus is visualized by an antibody against β-galactosidase. (**C**) Dorsomedial part of the OB on the same section shown in A and B. Counterstaining with DAPI. (**D**) After stimulation of the animal with pentadecanal, glomeruli in the dorsomedial part of the OB are surrounded by only a few c-Fos–positive cells. (**E**) Cross section through the more posterior region of the OB (600 μm distant from the one shown in A–D) of a mouse stimulated with pentadecanal. Counterstaining with DAPI. (**F**) In the contrast to the anterior–ventral domain, in the more posterior–ventral domain hardly any glomeruli with c-Fos–positive JCs were detectable. Scale bar: 100 μm in A–F. This figure appears in color in the online version of *Chemical Senses*.

experimental procedure allowed an identification of glomeruli, which are activated by such compounds and in turn, is a suitable approach in search for OR types, which are activated by them. This is of particular importance as these extremely hydrophobic molecules are supposed to be difficult to solubilize and might therefore not lead to receptor activation in heterologous expression systems (see Supplementary Figure 1). The location of glomeruli activated by long-chain alkanes in the ventral portion of the bulb (Figure 1) is in line with previous studies of rats using the $^{14}$C-deoxyglucose technique (Ho et al. 2006); thus suggesting a similar chemotopical organization of the OB in both species. The observation that none of the hitherto analyzed compounds in rats and mice led to activated glomeruli in the area of the OR37 glomeruli at the ventral midline of the bulb (Johnson et al. 1998, 1999, 2002, 2004; Xu et al. 2003) suggested that unique compounds are the ligands for OR37 receptors. This notion is in line with several unusual features of the OR37 receptor types.

The procedure that was used in this study has allowed for the first time to identify chemical compounds, which are able to activate JCs surrounding the glomerulus of distinct OR37 subtypes (Figure 4). Interestingly, in all cases, the active compounds turned out to be long-chain fatty aldehydes, which—to our knowledge—were never described as active ligands for ORs in any previous studies. This finding implies that the structurally unique OR37 receptors with their insertion in the E3 loop may be specifically tuned for recognizing long-chain fatty aldehydes. This view is supported by our observation that the related alcohols or acids had only little or no effects, respectively (Figure 8). The finding that aldehydes elicited stronger c-Fos expression at the OR37 glomeruli compared with the corresponding alcohols or acids may partly be due to the higher vapor pressure of the aldehydes. However, their physiochemical properties are most likely not entirely responsible for the observed differences in activation intensity because the alkanes induced no activation of the glomeruli but have an even higher vapor pressure

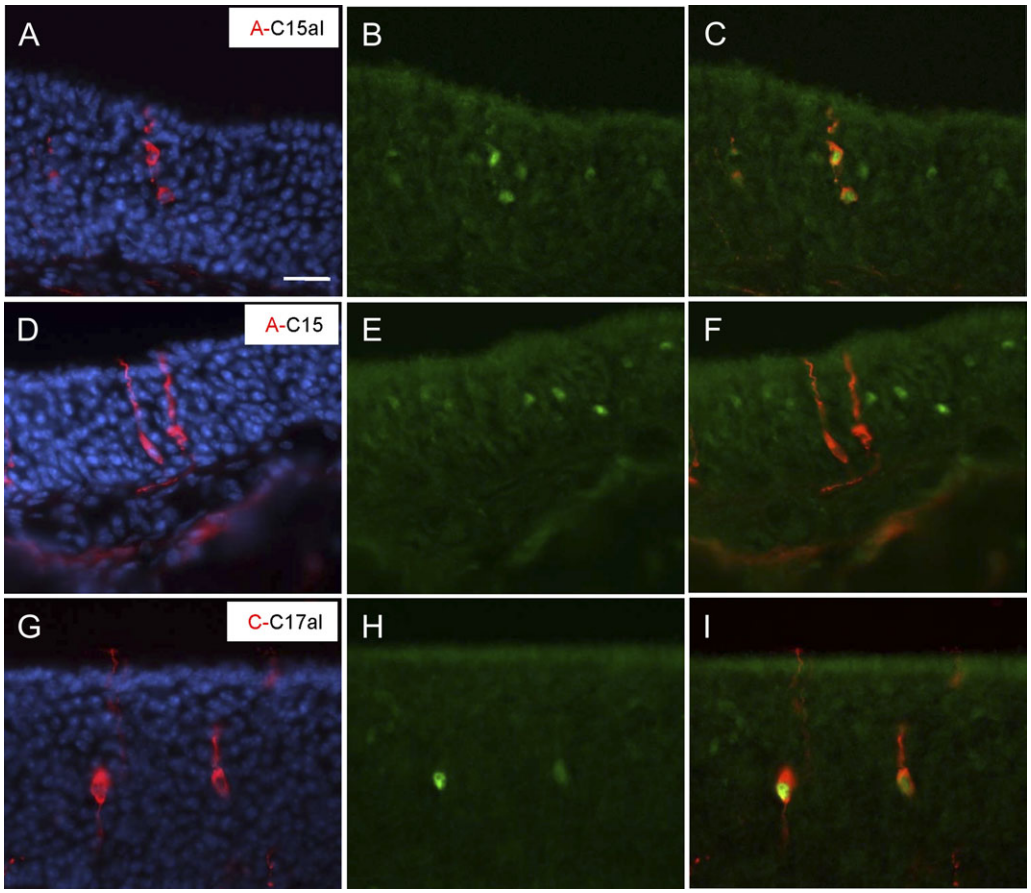


**Figure 10** Long-chain aldehydes induce c-Fos expression in OSNs expressing OR37 receptors. (**A**) Cross section through OE of an OR37A-ITlacZ mouse; OR37A expressing cells were visualized by an antibody against β-galactosidase. Counterstaining with DAPI. (**B**) Pentadecanal (C15al) elicits c-Fos expression in distinct cells within the OE. (**C**) An overlay of the c-Fos staining and OR37A immunoreactivity revealed that OR37A expressing OSNs were c-Fos positive. (**D**) Cross section through OE of an OR37A-ITlacZ mouse; OR37A expressing cells were visualized by an antibody against β-galactosidase. Counterstaining with DAPI. (**E**) Pentadecane (C15) elicits c-Fos expression in distinct cells within the OE. (**F**) An overlay of the c-Fos staining and OR37A immunoreactivity revealed that OR37A expressing OSNs were not c-Fos positive. (**G**) Cross section through OE of an OR37C-ITlacZ mouse; OR37C expressing cells were visualized by an antibody against β-galactosidase. Counterstaining with DAPI. (**H**) Heptadecanal (C17al) elicits c-Fos expression in distinct cells within the MOE. (**I**) An overlay of the c-Fos staining and the OR37C immunoreactivity revealed that OR37C expressing OSNs were c-Fos positive. Scale bar: 20μm in A–I. This figure appears in color in the online version of *Chemical Senses*.

than the aldehydes. The specificity that became apparent for the OR37 receptors when using these few compounds would be rather untypical for ORs and OSNs, which usually respond to a broader spectrum of chemical structures (Sato et al. 1994; Duchamp-Viret et al. 1999; Malnic et al. 1999; Araneda et al. 2000; Bozza et al. 2002; Mombaerts 2004; Grosmaitre et al. 2006; Malnic 2007; Touhara 2007; Saito et al. 2009). For the OR37 receptors, this feature seems to be extended to a different ligand specificity of each OR37 subtype, with OR37A responding preferentially to the C15 aldehyde, OR37B to the C16 aldehyde, and OR37C to the C17 aldehyde. In view of the concept that ORs with similar primary structure are supposed to interact with structurally related chemical compounds (Mori and Yoshihara 1995; Malnic et al. 1999), this finding is particularly striking, as all 3 OR37 subtypes share a very high degree of sequence identity (Hoppe et al. 2000). However, the result is in perfect accordance with the phylogenetic sequence conservation for each subtype (Hoppe et al. 2003, 2006), which has led to the speculation that the ligands for the OR37 subtypes may be of particular biological relevance. In the context of our previous finding that receptors of the OR37 family are exclusively found in mammalian species (Hoppe et al. 2006), the identification of long-chain fatty aldehydes as ligands for OR37 receptors is of particular relevance. Long-chain aliphatic compounds have been found as constituents in exocrine secretions of various mammalian species (Brooke and Decker 1996; Li et al. 1997; Wood 2003; Hayes et al. 2004; Zhang et al. 2008). There is currently no information available showing whether those fatty aldehydes, which we have identified as activators of OR37 glomeruli, are constituents of sebaceous secretions; however, this may just be

because they are not particularly enriched in this material. A low abundance of such compounds could argue in favor of their possible function as signaling molecules.

## Supplementary material

Supplementary material can be found at http://www.chemse.oxfordjournals.org/

## Funding

This work was supported by the Deutsche Forschungsgemeinschaft [grant BR712/23-1 to H.B. and J.S. and grants SFB 894 and INST 256/271-1 FUGG to F.Z. and B.B.].

## Acknowledgements

The authors would like to thank Diana Loch for her initial contribution to the work. We thank Dr W. Bettray, Institute of Organic Chemistry, Rheinisch-Westfälische Technische Hochschule Aachen for providing pentadecanal. We thank Prof. Dr Uwe Jensen, Institute of Applied Mathematics and Statistics, University of Hohenheim for his support in statistical analyses.

## References

Araneda RC, Kini AD, Firestein S. 2000. The molecular receptive range of an odorant receptor. Nat Neurosci. 3:1248–1255.

Ben Arie N, Lancet D, Taylor C, Khen M, Walker N, Ledbetter DH, Carrozzo R, Patel K, Sheer D, Lehrach H. 1994. Olfactory receptor gene cluster on human chromosome 17: possible duplication of an ancestral receptor repertoire. Hum Mol Genet. 3:229–235.

Bozza T, Feinstein P, Zheng C, Mombaerts P. 2002. Odorant receptor expression defines functional units in the mouse olfactory system. J Neurosci. 22:3033–3043.

Brooke AP, Decker DM. 1996. Lipid compounds in secretions of fishing bat, Noctilio leporinus (Chiroptera: Noctilionidea). J Chem Ecol. 22:1411–1428.

Buck L, Axel R. 1991. A novel multigene family may encode odorant receptors: a molecular basis for odor recognition. Cell. 65:175–187.

Bufe B, Hofmann T, Krautwurst D, Raguse JD, Meyerhof W. 2002. The human TAS2R16 receptor mediates bitter taste in response to beta-glucopyranosides. Nat Genet. 32:397–401.

Clarin T, Sandhu S, Apfelbach R. 2010. Odor detection and odor discrimination in subadult and adult rats for two enantiomeric odorants supported by c-fos data. Behav Brain Res. 206:229–235.

Duchamp-Viret P, Chaput MA, Duchamp A. 1999. Odor response properties of rat olfactory receptor neurons. Science. 284:2171–2174.

Fletcher ML, Masurkar AV, Xing J, Imamura F, Xiong W, Nagayama S, Mutoh H, Greer CA, Knopfel T, Chen WR. 2009. Optical imaging of postsynaptic odor representation in the glomerular layer of the mouse olfactory bulb. J Neurophysiol. 102:817–830.

Fried HU, Fuss SH, Korsching SI. 2002. Selective imaging of presynaptic activity in the mouse olfactory bulb shows concentration and structure dependence of odor responses in identified glomeruli. Proc Natl Acad Sci U S A. 99:3222–3227.

Frigerio M, Santagostino M. 1994. A mild oxidizing reagent for alcohols and 1,2-diols: o-iodoxybenzoic acid (IBX) in DMSO. Tetrahedron Lett. 35:8019–8022.

Frigerio M, Santagostino M, Sputore S. 1999. A user-friendly entry to 2-iodoxybenzoic acid (IBX). J Org Chem. 64:4537–4538.

Glusman G, Clifton S, Roe B, Lancet D. 1996. Sequence analysis in the olfactory receptor gene cluster on human chromosome 17: recombinatorial events affecting receptor diversity. Genomics. 37:147–160.

Godfrey PA, Malnic B, Buck LB. 2004. The mouse olfactory receptor gene family. Proc Natl Acad Sci U S A. 101:2156–2161.

Grosmaitre X, Vassalli A, Mombaerts P, Shepherd GM, Ma M. 2006. Odorant responses of olfactory sensory neurons expressing the odorant receptor MOR23: a patch clamp analysis in gene-targeted mice. Proc Natl Acad Sci U S A. 103:1970–1975.

Guthrie KM, Anderson AJ, Leon M, Gall C. 1993. Odor-induced increases in c-fos mRNA expression reveal an anatomical "unit" for odor processing in olfactory bulb. Proc Natl Acad Sci U S A. 90:3329–3333.

Hayes RA, Morelli TL, Wright PC. 2004. Anogenital gland secretions of Lemur catta and Propithecus verreauxi coquereli: a preliminary chemical examination. Am J Primatol. 63:49–62.

Ho SL, Johnson BA, Leon M. 2006. Long hydrocarbon chains serve as unique molecular features recognized by ventral glomeruli of the rat olfactory bulb. J Comp Neurol. 498:16–30.

Hoppe R, Breer H, Strotmann J. 2003. Organization and evolutionary relatedness of OR37 olfactory receptor genes in mouse and human. Genomics. 82:355–364.

Hoppe R, Lambert TD, Samollow PB, Breer H, Strotmann J. 2006. Evolution of the "OR37" subfamily of olfactory receptors: a cross-species comparison. J Mol Evol. 62:460–472.

Hoppe R, Weimer M, Beck A, Breer H, Strotmann J. 2000. Sequence analyses of the olfactory receptor gene cluster mOR37 on mouse chromosome 4 [in process citation]. Genomics. 66:284–295.

Igarashi KM, Mori K. 2005. Spatial representation of hydrocarbon odorants in the ventrolateral zones of the rat olfactory bulb. J Neurophysiol. 93:1007–1019.

Johnson BA, Farahbod H, Xu Z, Saber S, Leon M. 2004. Local and global chemotopic organization: general features of the glomerular representations of aliphatic odorants differing in carbon number. J Comp Neurol. 480:234–249.

Johnson BA, Ho SL, Xu Z, Yihan JS, Yip S, Hingco EE, Leon M. 2002. Functional mapping of the rat olfactory bulb using diverse odorants reveals modular responses to functional groups and hydrocarbon structural features. J Comp Neurol. 449:180–194.

Johnson BA, Woo CC, Hingco EE, Pham KL, Leon M. 1999. Multidimensional chemotopic responses to n-aliphatic acid odorants in the rat olfactory bulb. J Comp Neurol. 409:529–548.

Johnson BA, Woo CC, Leon M. 1998. Spatial coding of odorant features in the glomerular layer of the rat olfactory bulb. J Comp Neurol. 393:457–471.

Kubick S, Strotmann J, Andreini I, Breer H. 1997. Subfamily of olfactory receptors characterized by unique structural features and expression patterns. J Neurochem. 69:465–475.

Lane RP, Cutforth T, Young J, Athanasiou M, Friedman C, Rowen L, Evans G, Axel R, Hood L, Trask BJ. 2001. Genomic analysis of orthologous mouse and human olfactory receptor loci. Proc Natl Acad Sci U S A. 98:7390–7395.

Li G, Roze U, Locke DC. 1997. Warning odor of the North American porcupine (Erethizon dorsatum). J Chem Ecol. 23:2737–2757.

Lin DY, Shea SD, Katz LC. 2006. Representation of natural stimuli in the rodent main olfactory bulb. Neuron. 50:937–949.

Lin W, Arellano J, Slotnick B, Restrepo D. 2004. Odors detected by mice deficient in cyclic nucleotide-gated channel subunit A2 stimulate the main olfactory system. J Neurosci. 24:3703–3710.

Malnic B. 2007. Searching for the ligands of odorant receptors. Mol Neurobiol. 35:175–181.

Malnic B, Godfrey PA, Buck LB. 2004. The human olfactory receptor gene family. Proc Natl Acad Sci U S A. 101:2584–2589.

Malnic B, Hirono J, Sato T, Buck LB. 1999. Combinatorial receptor codes for odors. Cell. 96:713–723.

McGann JP, Pirez N, Wachowiak M. 2006. Imaging odor coding and synaptic plasticity in the mammalian brain with a genetically-encoded probe. Conf Proc IEEE Eng Med Biol Soc. 1:664–667.

Meister M, Bonhoeffer T. 2001. Tuning and topography in an odor map on the rat olfactory bulb. J Neurosci. 21:1351–1360.

Mizrahi A, Matsunami H, Katz LC. 2004. An imaging-based approach to identify ligands for olfactory receptors. Neuropharmacology. 47:661–668.

Mombaerts P. 2004. Genes and ligands for odorant, vomeronasal and taste receptors. Nat Rev Neurosci. 5:263–278.

Mombaerts P, Wang F, Dulac C, Chao SK, Nemes A, Mendelsohn M, Edmondson J, Axel R. 1996. Visualizing an olfactory sensory map. Cell. 87:675–686.

Mori K, Yoshihara Y. 1995. Molecular recognition and olfactory processing in the mammalian olfactory system. Prog Neurobiol. 45:585–619.

Oka Y, Katada S, Omura M, Suwa M, Yoshihara Y, Touhara K. 2006. Odorant receptor map in the mouse olfactory bulb: in vivo sensitivity and specificity of receptor-defined glomeruli. Neuron. 52:857–869.

Oliva AM, Jones KR, Restrepo D. 2008. Sensory-dependent asymmetry for a urine-responsive olfactory bulb glomerulus. J Comp Neurol. 510:475–483.

Ressler KJ, Sullivan SL, Buck LB. 1993. A zonal organization of odorant receptor gene expression in the olfactory epithelium. Cell. 73:597–609.

Ressler KJ, Sullivan SL, Buck LB. 1994. Information coding in the olfactory system: evidence for a stereotyped and highly organized epitope map in the olfactory bulb. Cell. 79:1245–1255.

Saito H, Chi Q, Zhuang H, Matsunami H, Mainland JD. 2009. Odor coding by a mammalian receptor repertoire. Sci Signal. 2:ra9.

Salcedo E, Zhang C, Kronberg E, Restrepo D. 2005. Analysis of training-induced changes in ethyl acetate odor maps using a new computational tool to map the glomerular layer of the olfactory bulb. Chem Senses. 30:615–626.

Sato T, Hirono J, Tonoike M, Takebayashi M. 1994. Tuning specificities to aliphatic odorants in mouse olfactory receptor neurons and their local distribution. J Neurophysiol. 72:2980–2989.

Sosinsky A, Glusman G, Lancet D. 2000. The genomic structure of human olfactory receptor genes. Genomics. 70:49–61.

Spors H, Grinvald A. 2002. Spatio-temporal dynamics of odor representations in the mammalian olfactory bulb. Neuron. 34:301–315.

Strotmann J, Conzelmann S, Beck A, Feinstein P, Breer H, Mombaerts P. 2000. Local permutations in the glomerular array of the mouse olfactory bulb. J Neurosci. 20:6927–6938.

Strotmann J, Hoppe R, Conzelmann S, Feinstein P, Mombaerts P, Breer H. 1999. Small subfamily of olfactory receptor genes: structural features, expression pattern and genomic organization. Gene. 236:281–291.

Strotmann J, Wanner I, Helfrich T, Beck A, Meinken C, Kubick S, Breer H. 1994. Olfactory neurones expressing distinct odorant receptor subtypes are spatially segregated in the nasal neuroepithelium. Cell Tissue Res. 276:429–438.

Takahashi YK, Kurosaki M, Hirono S, Mori K. 2004. Topographic representation of odorant molecular features in the rat olfactory bulb. J Neurophysiol. 92:2413–2427.

Thody AJ, Shuster S. 1989. Control and function of sebaceous glands. Physiol Rev. 69:383–416.

Touhara K. 2007. Deorphanizing vertebrate olfactory receptors: recent advances in odorant-response assays. Neurochem Int. 51:132–139.

Vassar R, Chao SK, Sitcheran R, Nunez JM, Vosshall LB, Axel R. 1994. Topographic organization of sensory projections to the olfactory bulb. Cell. 79:981–991.

Vassar R, Ngai J, Axel R. 1993. Spatial segregation of odorant receptor expression in the mammalian olfactory epithelium. Cell. 74:309–318.

Wachowiak M, Cohen LB. 2003. Correspondence between odorant-evoked patterns of receptor neuron input and intrinsic optical signals in the mouse olfactory bulb. J Neurophysiol. 89:1623–1639.

Wood WF. 2003. Volatile components in metatarsal glands of sika deer, Cervus nippon. J Chem Ecol. 29:2729–2733.

Xie SY, Feinstein P, Mombaerts P. 2000. Characterization of a cluster comprising approximately 100 odorant receptor genes in mouse. Mamm Genome. 11:1070–1078.

Xu F, Liu N, Kida I, Rothman DL, Hyder F, Shepherd GM. 2003. Odor maps of aldehydes and esters revealed by functional MRI in the glomerular layer of the mouse olfactory bulb. Proc Natl Acad Sci U S A. 100:11029–11034.

Young JM, Trask BJ. 2002. The sense of smell: genomics of vertebrate odorant receptors. Hum Mol Genet. 11:1153–1160.

Zhang JX, Sun L, Zhang JH, Feng ZY. 2008. Sex- and gonad-affecting scent compounds and 3 male pheromones in the rat. Chem Senses. 33:611–621.

Zhang X, Firestein S. 2002. The olfactory receptor gene superfamily of the mouse. Nat Neurosci. 5:124–133.

Zhuang H, Matsunami H. 2007. Synergism of accessory factors in functional expression of mammalian odorant receptors. J Biol Chem. 282:15284–15293.